Supporting Information for "Latitudinal beaming of Jupiter's radio emissions from Juno/Waves flux density measurements"

C. K. Louis[1,2,3], P. Zarka[2], K. Dabidin[2], P.-A. Lampson[2], F. P. Magalhães[2],

A. Boudouma[2], M. S. Marques[4]and B. Cecconi[2]

[1]School of Cosmic Physics, DIAS Dunsink Observatory, Dublin Institute for Advanced Studies, Dublin 15, Ireland

[2]LESIA, Observatoire de Paris, PSL Research University, CNRS, Sorbonne Universités, UPMC Univ. Paris 06, Univ. Paris Diderot, Sorbonne Paris Cité, Meudon, France

[3]Institut de Recherche en Astrophysique et Plantologie (IRAP), Universit de Toulouse, CNRS, CNES, UPS, (Toulouse), France

[4]Departamento de Geofsica, Universidade Federal do Rio Grande do Norte, Natal, RN, Brazil

Contents of this file:

Introduction

These Supporting Information contain details on the data processing and the latitudinal distribution study.

Table S1 - Intensity threshold for each component and each frequency channel

Table S1. gives the processed intensity thresholds (in $V^2/m^2/Hz$) for each Jovian radio component and each frequency covered by this component, that separates the Gaussian noise distribution from the tail of higher intensity values characterizing the corresponding component (see. Figure S2).

Figure S1 - Calibrated reference spectra

Figure S1 shows the reference spectra calibrated in flux densities, used to build the bandpass response curve of the Juno/Waves instrument. Diamonds are the smoothed median 50% and 1% spectra derived from Cassini radio observations (Figures 7a,b of Zarka et al., 2004). The Jovian radio spectrum derived from Voyager radio observations between 0.5 and 40.5 MHz in (Zarka, 1992) matches well the median 1% Cassini curve. The upper black curve is the overall reference 1% spectrum deduced from Cassini+Voyager observations, and extrapolated below 3.5 kHz (down to 1 kHz) following the curvature of the lower part of the spectrum, and also consistent with the spectral shape observed in the LFR-low band of Juno/Waves. The lower red curve is the overall reference 50% spectrum adjusted from the corresponding Cassini data, complemented by the Voyager spectrum downscaled to match the 0.5 - 6.5 MHz range. The spectrum turnover below 5 kHz has been overlooked for better matching the spectral shape of the 1% Cassini spectrum and the spectrum shape observed in the LFR-low band of Juno/Waves. These 2 curves are reproduced as the dashed spectra in Figure A4c.

Figure S2 - Automatic threshold for each component, at each frequency channel

Figure S2 displays the histograms of processed intensities for 3 selected Jovian radio components and frequencies (corresponding to the 3 columns). In each case, the measured histogram is displayed in black (with linear scale on top panel, logarithmic scale in the bottom panel). The red curve is the Gaussian fits to the left-hand part of each distribution, below its maximum, then symmetrized. A higher intensity tail is visible in each case above the threshold indicated by the dashed line, automatically computed for each plot. The

thresholds for all components and all corresponding radio frequencies are tabulated in Table S1.

Figure S3 - Centrifugal Latitudinal distribution of the occurrence of each components

Figures S3 shows the occurrence distribution of each radio component, as a function of Centrifugal Latitude and frequency.

Figure S4 - Jovicentric Latitudinal distribution of the occurrence of each components

Figures S4 shows the occurrence distribution of each radio component, as a function of Jovicentric Latitude and frequency.

Table S1. Intensity threshold for each component and each frequency channel.

Frequency (kHz)	Threshold value ($V^2/m^2/Hz$) QP	nLF	nKOM	bKOM	Frequency (kHz)	Threshold value ($V^2/m^2/Hz$) DAM	Io
1.00100	2.704E-14			1.202E-13	3500.000	1.491E-18	3.613E-18
1.12300	1.970E-14			1.877E-14	4500.000	3.675E-18	7.852E-18
1.26950	1.291E-14			1.156E-14	5500.000	1.794E-18	6.781E-18
1.41600	1.169E-14			2.441E-14	6500.000	2.229E-18	4.417E-18
1.58690	8.175E-15			1.226E-14	7500.000	4.042E-18	5.944E-18
1.78220	5.559E-15	7.339E-16		5.366E-15	8500.000	1.145E-17	1.199E-17
2.00200	3.843E-15	9.047E-15		3.095E-15	9500.000	2.854E-18	5.046E-18
2.24610	2.908E-15	8.350E-16		1.466E-15	10500.00	2.367E-18	4.462E-18
2.51470	1.655E-15	4.784E-15		9.937E-16	11500.00	2.154E-18	7.790E-18
2.83200	1.107E-15	1.057E-15		4.880E-16	12500.00	6.752E-18	8.457E-18
3.17380	7.882E-16	1.858E-15		4.480E-16	13500.00	2.228E-17	1.006E-17
3.54000	4.810E-16	2.685E-15		1.145E-15	14500.00	3.863E-17	6.383E-18
3.97950	2.998E-16	3.496E-16		1.956E-16	15500.00	3.373E-18	8.058E-18
4.46780	5.438E-16	3.300E-16		8.723E-16	16500.00	9.229E-18	1.947E-16
5.00490	1.261E-16	2.629E-16		2.128E-16	17500.00	3.272E-18	8.407E-18
5.61520	1.011E-16	9.053E-17		1.900E-15	18500.00	3.077E-18	5.673E-18
6.29880	7.184E-17	8.823E-17		6.456E-17	19500.00	8.499E-18	1.472E-17
7.08010	5.927E-17	1.632E-16		5.168E-17	20500.00	1.057E-17	8.946E-18
7.95900	4.837E-17	3.764E-16		4.523E-16	21500.00	1.750E-17	1.400E-17
8.93550	4.013E-17	1.071E-16		4.578E-16	22500.00	8.181E-18	1.146E-17
10.0100	3.184E-17	1.336E-16		4.032E-16	23500.00	9.684E-18	1.642E-17
11.2300	2.575E-17	7.052E-17		2.866E-16	24500.00	8.739E-17	1.947E-17
12.6220	2.527E-17	6.168E-17	8.030E-17	2.529E-16	25500.00	1.323E-17	1.401E-17
14.1600	1.872E-17	3.829E-17	1.080E-16	1.710E-16	26500.00	1.089E-17	9.659E-18
15.8690	1.340E-17	4.958E-17	1.101E-16	1.340E-16	27500.00	1.353E-17	2.227E-17
17.7980	1.290E-17	1.318E-17	1.574E-16	1.313E-16	28500.00	1.037E-17	8.343E-18
19.9710	8.853E-18	1.061E-17	1.310E-17	1.084E-16	29500.00	8.158E-18	2.398E-17
19.9580	8.802E-18	2.920E-17	8.929E-18	6.794E-17	30500.00	1.696E-17	1.139E-17
22.3390	9.273E-17	1.251E-17	7.735E-18	6.676E-17	31500.00	5.712E-18	4.299E-18
25.0850	3.968E-17	1.149E-17	5.109E-18	6.659E-17	32500.00	8.464E-17	1.399E-17
28.1980	4.404E-18	1.664E-18	2.883E-17	4.309E-17	33500.00	7.839E-18	6.682E-18
31.6770	6.231E-18	9.362E-18	5.454E-18	4.340E-17	34500.00	6.412E-18	1.284E-18
35.5220	4.089E-18	1.250E-18	1.451E-17	3.073E-17	35500.00	6.016E-18	1.070E-18
39.9170	2.141E-18	2.657E-18	3.627E-18	2.562E-17	36500.00	3.019E-18	1.232E-18
44.8610	2.845E-18	4.030E-18	3.231E-18	2.082E-17	37500.00	1.685E-18	1.239E-18
50.1710	9.983E-19	2.759E-18	9.601E-18	1.690E-17	38500.00	1.437E-18	8.155E-20
56.2130	1.113E-18	5.136E-19	1.155E-17	1.848E-17	39500.00	6.937E-19	1.082E-18
63.1710	3.255E-19	1.233E-17	1.154E-17	9.634E-18	40500.00	2.297E-19	
70.8620	1.218E-19	1.126E-16	1.414E-17	1.121E-17			
79.4680	2.029E-19	4.030E-17	1.251E-17	5.774E-18			
89.1720	1.884E-19	3.331E-17	1.010E-17	7.512E-18			
100.160	2.637E-20	2.785E-17	9.338E-17	1.088E-17			
112.430	6.714E-20		1.161E-17	6.757E-18			
126.160	6.983E-20		1.741E-17	7.732E-18			
141.540	2.130E-19		7.85[illegible]	1.689E-17			

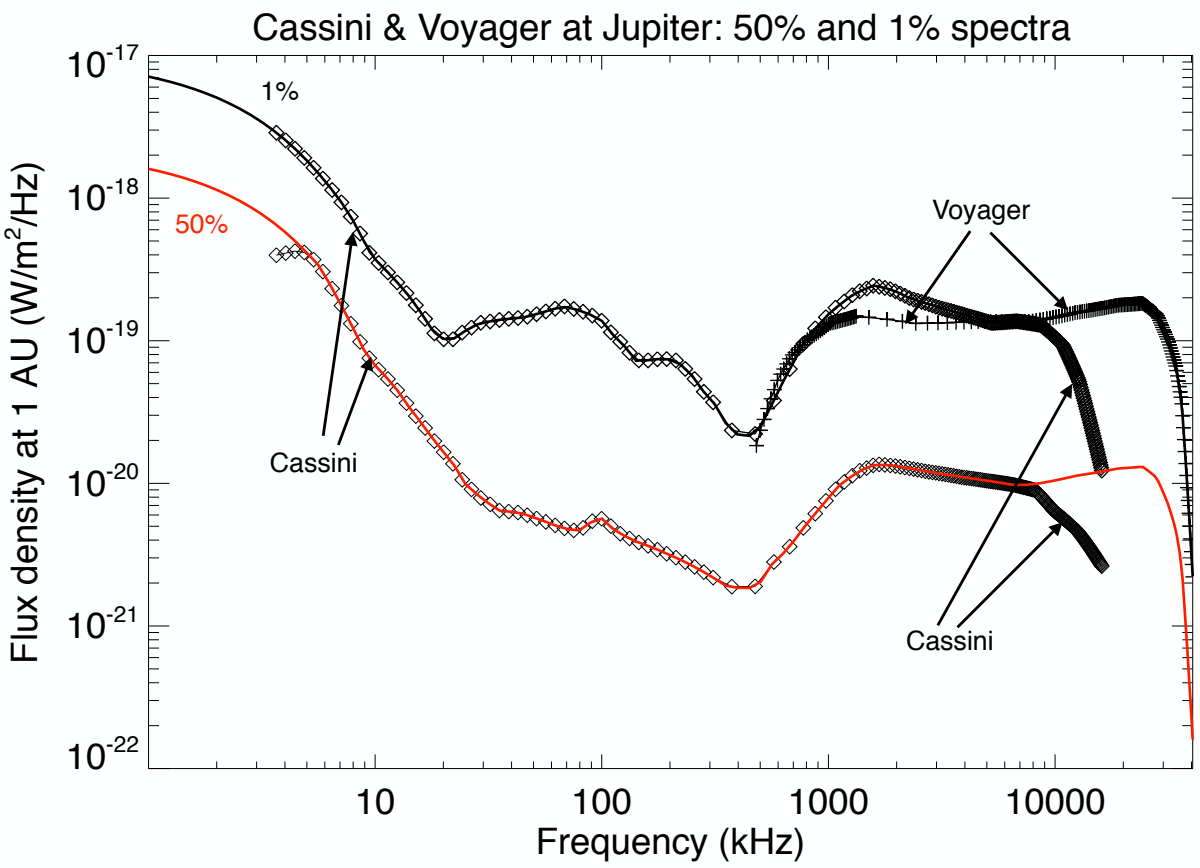

Figure S1. Calibrated reference spectra.

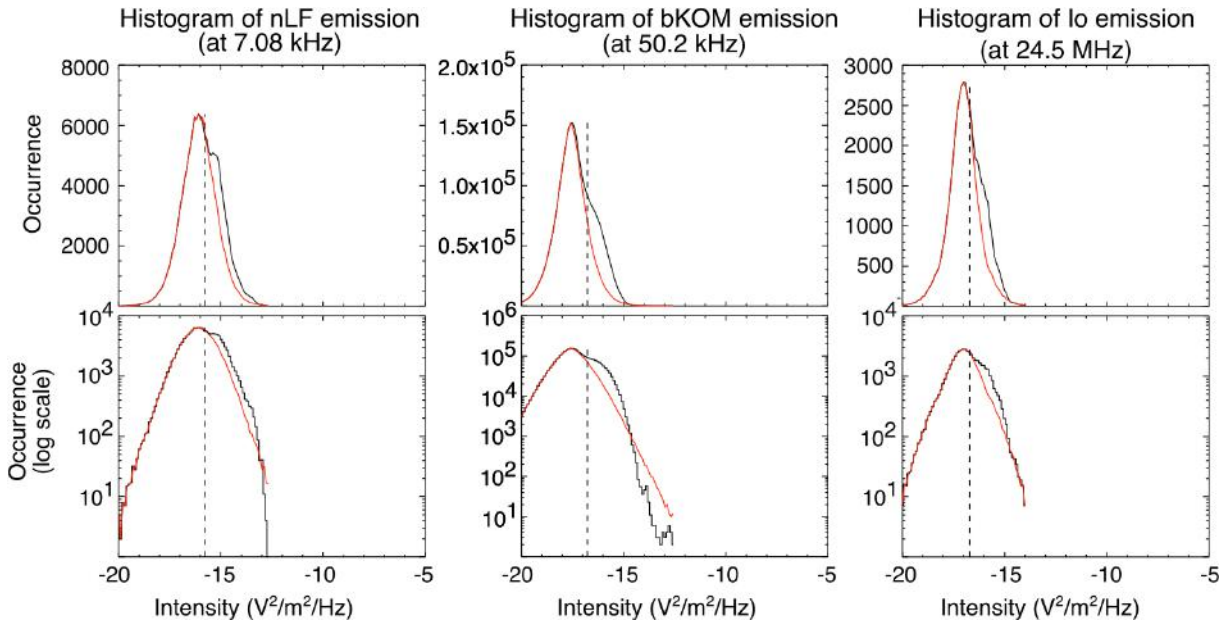

Figure S2. Histograms for threshold determination.

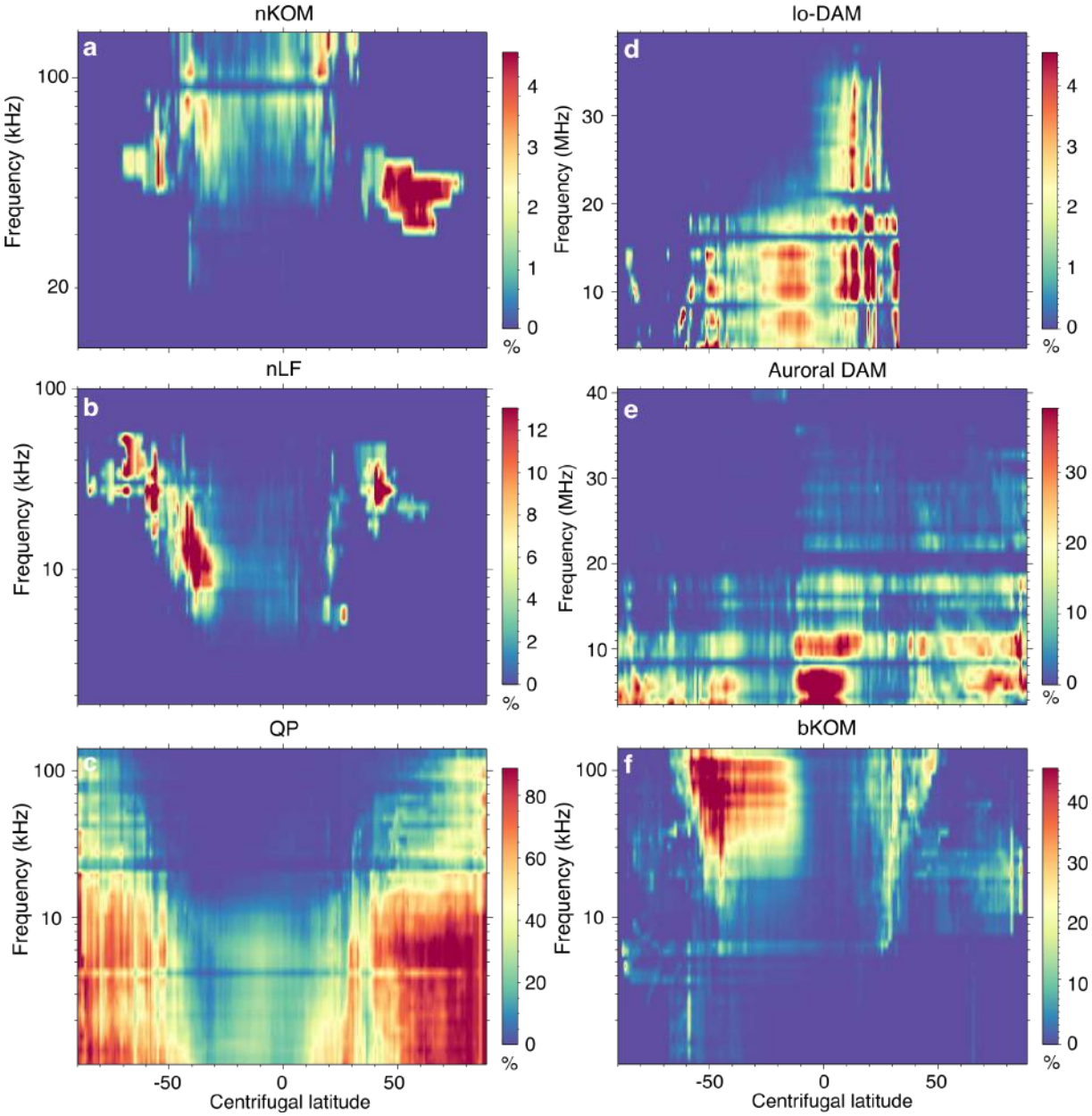

Figure S3. Distribution of the occurrence of each component in Centrifugal Latitude. Same as Figure 3, but versus Centrifugal latitude and frequency.

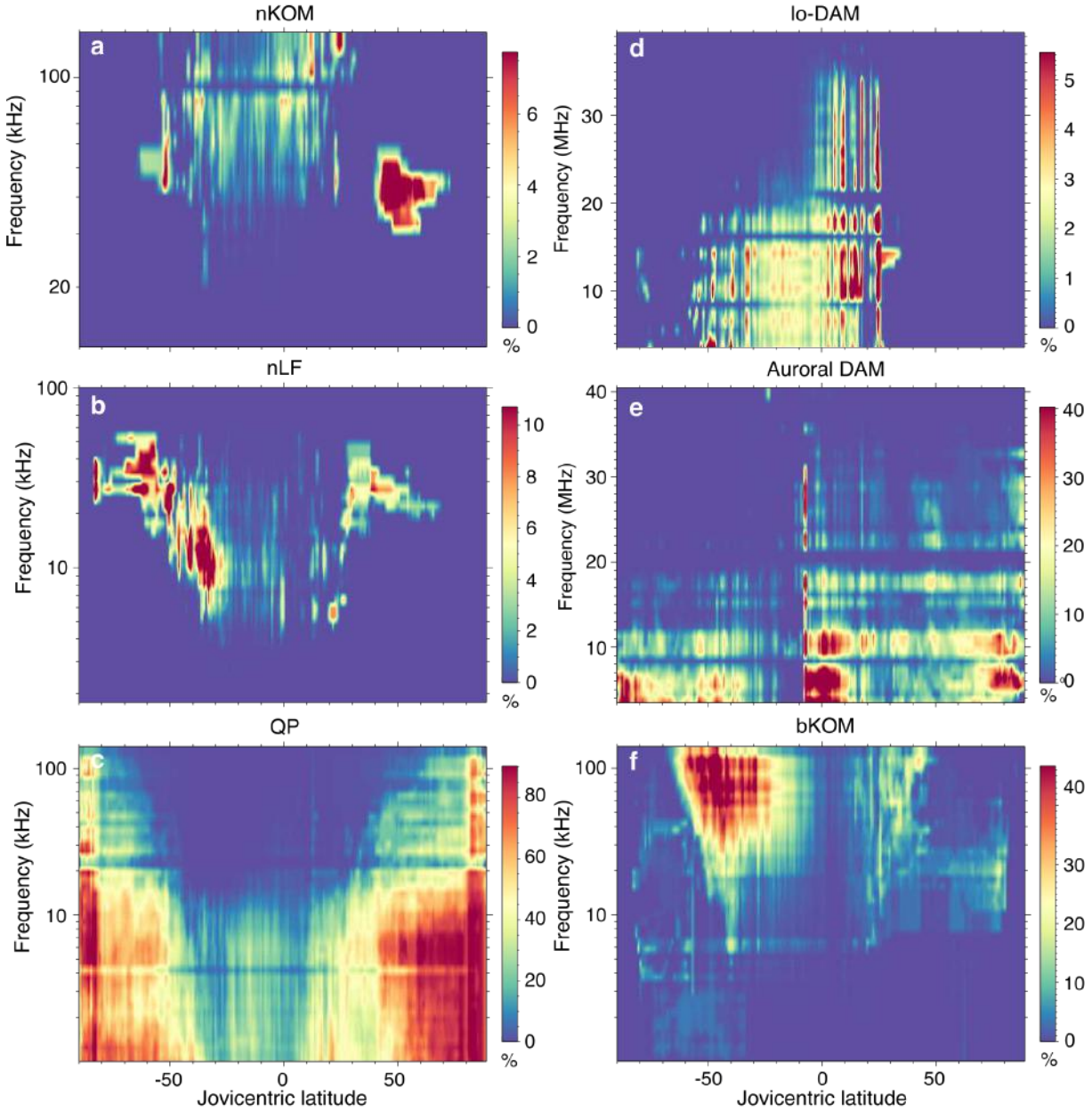

Figure S4. Distribution of the occurrence of each component in Jovicentric Latitude. Same as Figure 3, but versus Jovicentric latitude and frequency.